European Journal of Phycology

ISSN: 0967-0262 (Print) 1469-4433 (Online) Journal homepage: http://www.tandfonline.com/loi/tejp20

Ultrastructure and molecular phylogenetic position of a new marine sand-dwelling dinoflagellate from British Columbia, Canada: Pseudadenoides polypyrenoides sp. nov. (Dinophyceae)

Mona Hoppenrath, Naoji Yubuki, Rowena Stern & Brian S. Leander

To cite this article: Mona Hoppenrath, Naoji Yubuki, Rowena Stern & Brian S. Leander (2017) Ultrastructure and molecular phylogenetic position of a new marine sand-dwelling dinoflagellate from British Columbia, Canada: Pseudadenoides polypyrenoides sp. nov. (Dinophyceae), European Journal of Phycology, 52:2, 208-224, DOI: 10.1080/09670262.2016.1274788

To link to this article: http://dx.doi.org/10.1080/09670262.2016.1274788

EUROPEAN JOURNAL OF PHYCOLOGY, 2017
VOL. 52, NO. 2, 208–224
http://dx.doi.org/10.1080/09670262.2016.1274788

Ultrastructure and molecular phylogenetic position of a new marine sand-dwelling dinoflagellate from British Columbia, Canada: *Pseudadenoides polypyrenoides* sp. nov. (Dinophyceae)

Mona Hoppenrath[a,b], Naoji Yubuki[a,c], Rowena Stern[a,d] and Brian S. Leander[a]

[a]Departments of Botany and Zoology, University of British Columbia, 6270 University Boulevard, Vancouver, BC, V6T 1Z4, Canada; [b]Current address: Senckenberg am Meer, Deutsches Zentrum für Marine Biodiversitätsforschung (DZMB), Südstrand 44, Wilhelmshaven, Germany; [c]Current address: Departments of Parasitology and Zoology, Faculty of Science, Charles University, Vinicna 7, Prague, 128 44, Czech Republic; [d]Current address: Sir Alister Hardy Foundation for Ocean Science, The Laboratory, Citadel Hill, Plymouth PL1 2PB, UK

ABSTRACT

Two monospecific genera of marine benthic dinoflagellates, *Adenoides* and *Pseudadenoides*, have unusual thecal tabulation patterns (lack of cingular plates in the former; and no precingular plates and a complete posterior intercalary plate series in the latter) and are thus difficult to place within a phylogenetic framework. Although both genera share morphological similarities, they have not formed sister taxa in previous molecular phylogenetic analyses. We discovered and characterized a new species of *Pseudadenoides, P. polypyrenoides* sp. nov., at both the ultrastructural and molecular phylogenetic levels. Molecular phylogenetic analyses of SSU and LSU rDNA sequences demonstrated a close relationship between *P. polypyrenoides* sp. nov. and *Pseudadenoides kofoidii*, and *Adenoides* and *Pseudadenoides* formed sister taxa in phylogenetic trees inferred from LSU rDNA sequences. Comparisons of morphological traits, such as the apical pore complex (APC), demonstrated similarities between *Adenoides, Pseudadenoides* and several planktonic genera (e.g. *Heterocapsa, Azadinium* and *Amphidoma*). Molecular phylogenetic analyses of SSU and LSU rDNA sequences also demonstrated an undescribed species within *Adenoides.*

ARTICLE HISTORY Received 23 September 2016; Revised 23 November 2016; Accepted 3 December 2016

KEYWORDS Benthic; morphology; phylogeny; *Pseudadenoides kofoidii*; taxonomy; ultrastructure

Introduction

Herdman (1922) described two *Amphidinium* species characterized by their depressed, small episome: *A. eludens* and *A. kofoidii. Amphidinium kofoidii* is round to square in shape with a striking starch-ring in the middle of the cell (Herdman, 1922, fig. 2). *Amphidinium eludens* Herdman is more oval with an inconspicuous episome and a bulge in the sulcal region (Herdman, 1922, fig. 1). Balech (1956) described the new thecate genus *Adenoides*, with *A. eludens* (Herdman) Balech as the type. Hoppenrath *et al.* (2003) re-investigated and revised the description of *Adenoides eludens* and discussed the taxonomical problem caused by the basionym selection from Balech in detail. *Amphidinium kofoidii* Herdman would have been the correct basionym as the described species *Adenoides eludens* was morphologically conspecific with it. Whether the second species (*Amphidinium eludens*) described by Herdman (1922) really exists was not clear until recently (Hoppenrath *et al.*, 2014), aside from a brief textual account on the observation by Dodge & Lewis (1986). Gómez *et al.* (2015) discovered a new thecate taxon that under the light microscope looked like *Amphidinium eludens*. This new genus was morphologically different from *Adenoides* and also distinct at the molecular phylogenetic level (Gómez *et al.*, 2015). The formal description of this genus was complicated because nomenclatural problems had to be solved. In accordance with the ICN (International Code of Nomenclature for Algae, Fungi, and Plants; McNeill *et al.*, 2012), *Adenoides* has been redefined based on the emended description of the basionym *Amphidinium eludens* (Gómez *et al.*, 2015) and the new combination *Pseudadenoides kofoidii* (Herdman) F.Gómez, R. Onuma, Artigas & T.Horiguchi has been proposed to accommodate *Amphidinium kofoidii* (*Adenoides eludens sensu* Balech, 1956).

Both *Adenoides* and *Pseudadenoides* have very unusual thecal tabulation patterns (Hoppenrath *et al.*, 2003; Gómez *et al.*, 2015), and the designation of plates, especially of the cingular and sulcal plates, depends largely on interpretation (summarized for *P. kofoidii* in Hoppenrath *et al.*, 2003). *Pseudadenoides* lacks a precingular plate series, a feature only known from the also benthic genus

CONTACT Mona Hoppenrath mhoppenrath@senckenberg.de.

Plagiodinium Faust & Balech (Faust & Balech, 1993; Hoppenrath *et al.*, 2014). The classification of *Pseudadenoides* (as *Adenoides*) is still uncertain (Hoppenrath *et al.*, 2003; not listed by Hoppenrath in Adl *et al.*, 2012). Molecular phylogenetic analyses have shown *Pseudadenoides* (as *Adenoides*) to branch as the sister lineage to the *Prorocentrum* clade (e.g. Zhang *et al.*, 2007; Hoppenrath & Leander, 2008; Orr *et al.*, 2012; Hoppenrath *et al.*, 2013), a relationship that is important for understanding character evolution in core dinoflagellates (Hoppenrath *et al.*, 2013, 2014).

A diversity survey using mitochondrial COI (cytochrome oxidase I) gene sequences revealed that *Pseudadenoides* (as *Adenoides*) also occurred in a plankton sample from Saanich Inlet (British Columbia, Canada) at 10 m depth (Stern *et al.*, 2010), suggesting that the habitat distributions and species diversity within the genus is currently poorly understood.

During our survey of species diversity in marine sandy sediments in British Columbia, Canada, we discovered and characterized a second *Pseudadenoides* species at both the ultrastructural and molecular phylogenetic levels.

Materials and methods

Sampling

Sand samples were collected with a spoon during low tide at Centennial Beach, Boundary Bay, British Columbia, Canada during the years 2005 to 2007 (Supplementary Table 1). *Pseudadenoides polypyrenoides* sp. nov. occurred together with *P. kofoidii* in most samples.

Sand samples were transported directly to the laboratory, and the flagellates were separated from the sand by extraction through a fine filter (mesh size 45 μm) using melting seawater-ice (Uhlig, 1964). The flagellates accumulated in a Petri dish beneath the filter and were then identified at ×40 to ×250 magnifications. Cells were isolated by micropipetting for the differential interference contrast (DIC) light microscopy and culture establishment as described below.

Culturing

Isolated cells (sample taken 9 May 2005) were washed in filtered seawater and transferred into a Petri dish containing f/2-medium (Guillard & Ryther, 1962). After establishment of the unialgal culture it was maintained in tissue flasks at 17°C under low light conditions in f/2-medium. Unfortunately, the culture died shortly after our first electron microscopical preparations at the end of 2007.

Light and electron microscopy

Cells were observed directly and micromanipulated with a Leica DMIL inverted microscope (Wetzlar, Germany). For DIC light microscopy, isolated cells were placed on a glass specimen slide and covered with a cover slip. Images were produced with a Zeiss Axioplan 2 imaging microscope (Carl-Zeiss, Oberkochen, Germany) connected to a Leica DC500 colour digital camera.

For scanning electron microscopy (SEM), a part of the culture was fixed with several drops of acidic Lugol's solution overnight at room temperature. Cells were transferred onto a polycarbonate membrane filter (Corning Separations Div., Acton, Massachusetts, USA) with 5 μm pore size, washed with distilled water, dehydrated with a graded series of ethanol (30, 50, 70, 80, 95, 100%) and 100% hexamethyldisilazane (HMDS) at the end, and air dried. Filters were mounted on stubs, sputter-coated with gold and viewed under a Hitachi S4700 Scanning Electron Microscope (Hitachi High-Technologies Corporation, Tokyo, Japan). SEM images were presented on a black background using Adobe Photoshop CS6.

For transmission electron microscopy of *Pseudadenoides polypyrenoides*, cells were mixed with the same volume of fixative solution containing 4% glutaraldehyde in 0.2 M sodium cacodylate buffer (pH 7.2) at room temperature for 1 h. Cells were aggregated into a pellet by centrifugation at 1000 g for 5 min and rinsed with the buffer three times. These were then post-fixed in 1% OsO_4 in 0.2 M sodium cacodylate buffer at room temperature for 2 h followed by dehydration through an ethanol series (30, 50, 70, 80, 90, 95, 100%). Ethanol was replaced by 100% acetone before infiltrated with acetone-Epon 812 resin mixtures and 100% Epon 812 resin. Ultrathin sections were cut on a Leica EM UC6 ultramicrotome (Leica Microsystems, Wetzlar, Germany) and double-stained with 2% uranyl acetate and lead citrate (Reynolds, 1963). Ultrathin sections were observed using a Hitachi H7600 transmission electron microscope (Hitachi High-Technologies Corporation, Tokyo, Japan).

DNA extraction and polymerase chain reaction (PCR)

The cultures of *Pseudadenoides* species and additional cultured species (called *Adenoides eludens*) were obtained from the National Centre for Marine Algae and Microbiota (NCMA, formerly CCMP, Maine, USA) and the Microbial Culture Collection at National Institute for Environmental Studies (NIES, Tsukuba, Japan). Fifteen ml of culture were used for DNA extractions using a

DNeasy plant mini kit (Qiagen, Mississauga, Ontario, Canada) according to the manufacturer's instructions. PCR amplification was carried out using Puretaq Ready-To-Go PCR beads (GE Lifesciences, New Jersey, USA) and Jumpstart Redtaq ReadyMix Reaction mix (Sigma-Aldrich, St. Louis, Missouri, USA) using 0.4 µmol (final concentration) of each primer (according to manufacturer's instructions) in either 25 or 50 µl reactions. Amplification of large subunit (LSU) rDNA sequences was carried out using forward primers D1R or D3a (Scholin *et al.*, 1994) and reverse primer LSU-R2 (Takano & Horiguchi, 2006). Sequencing reactions were performed with these primers and with the reverse primer LSU-25R1 (Takano & Horiguchi, 2006). Amplifications of small subunit (SSU) rDNA sequencing reactions were performed with the forward primer UPro18SF and the reverse primer U18R (Hong *et al.*, 2008). Sequencing reactions were performed with these primers and the universal primers EK555F (forward) and EK1269R (reverse) (Lòpez-García *et al.*, 2001). Residual primers were removed from PCR reactions using the ExoSAPIT reagent (Affymetrix, USA). Sequencing was performed by Macrogen (Korea) and Source Bioscience (Nottingham, UK).

Sequence alignments and phylogenetic analysis

Partial DNA sequences were manually checked for errors, and constructed to their full length using BioEdit (Hall, 1999). Additionally the sequences were checked for their correct identity as either *Pseudadenoides* or *Adenoides* by the BLASTn algorithm (Altschul *et al.*, 1990). SSU and LSU rDNA sequences were automatically aligned using MAFFT with L-INS-i option (Katoh *et al.*, 2005; Katoh & Standley, 2013), as recommended for an analysis of a small alignment like this dataset. The two different datasets were then manually aligned and trimmed to exclude all ambiguous sites using Mesquite version 3.04 (Maddison & Maddison, 2015). The final datasets used in the analysis contained 64 taxa and 1564 unambiguously aligned sites for the SSU rDNA dataset, and 51 taxa and 1011 unambiguously aligned sites for the LSU rDNA dataset.

The phylogenetic trees were inferred using Maximum Likelihood (ML) with the program Garli 2.0 (Zwickl, 2006) under a GTR + I + G model for the SSU rDNA dataset and a TIM2 + I + G for the LSU rDNA dataset, both of which were selected by jModeltest 2.1.6 (Darriba *et al.*, 2012). ML bootstrap analyses were carried out with 1000 pseudoreplicates. Bayesian analyses using MrBayes v3.2.5 (Ronquist *et al.*, 2011) was performed on two independent groups of four Monte-Carlo-Markov Chains (MCMC), starting from random trees. A total of 1 000 000 MCMC generations were run, and the trees were sampled every 500th generation. The first 25% of the generations were discarded as burn-in. Posterior probabilities (PP) were calculated from the sampling points.

Results

Pseudadenoides polypyrenoides *Hoppenrath, Yubuki, R. Stern & B. S. Leander, sp. nov. (Figs 1–3, 7–24, 37–51)*

Description: Thecate species with laterally flattened, asymmetrical cells with the dorsal side of the posterior end longer. Button-like epitheca and large hypotheca with complete, not displaced, shallow anterior cingulum and very short sulcus. Plate formula: APC 4′′ 6C 4S 5′′′ 5p 1′′′′. No precingular plate series. Complete posterior intercalary plate series. Three large pores containing small sieve-like pores on the dorsal side of the posterior end of the cell, one each on plates 3p, 4p and 1′′′′. Specimens 28.8–38.3 µm long and 25.6–34.0 µm deep. Central nucleus. Typical dinoflagellate chloroplasts with several stalked pyrenoids.

Holotype: Specimen shown in Fig. 10, conserved on SEM stub designated CEDiT2016H55 deposited in the Centre of Excellence for Dinophyte Taxonomy, Senckenberg am Meer, Wilhelmshaven, Germany.

Sequences: Nearly complete SSU and partial LSU rDNA sequences (GenBank accession numbers: KU726886 and KU726887).

Type Locality: Boundary Bay, British Columbia, Canada (49°0.0′N, 123°8.0′W).

Etymology: *polypyrenoides* in Greek, meaning several pyrenoids in contrast to only two large pyrenoids in *Pseudadenoides kofoidii.*

General morphology

Cells were asymmetrically oval, longer dorsal than ventral, and flattened laterally (Figs 1–3). Specimens were 28.8–38.3 µm long and 25.6–34.0 µm deep (n = 11) and ~24 to 25 µm wide (n = 2). The button-like epitheca was inconspicuous (Figs 1–3, 7–16). The cingulum completely encircled the epitheca, was not displaced, was very slightly depressed, and was located at the anterior end of the cell (Figs 9, 10, 12–14, 17–19). The slightly depressed sulcus was located in the anterior third of the cell, neither extending onto the epitheca nor reaching the posterior end of the cell

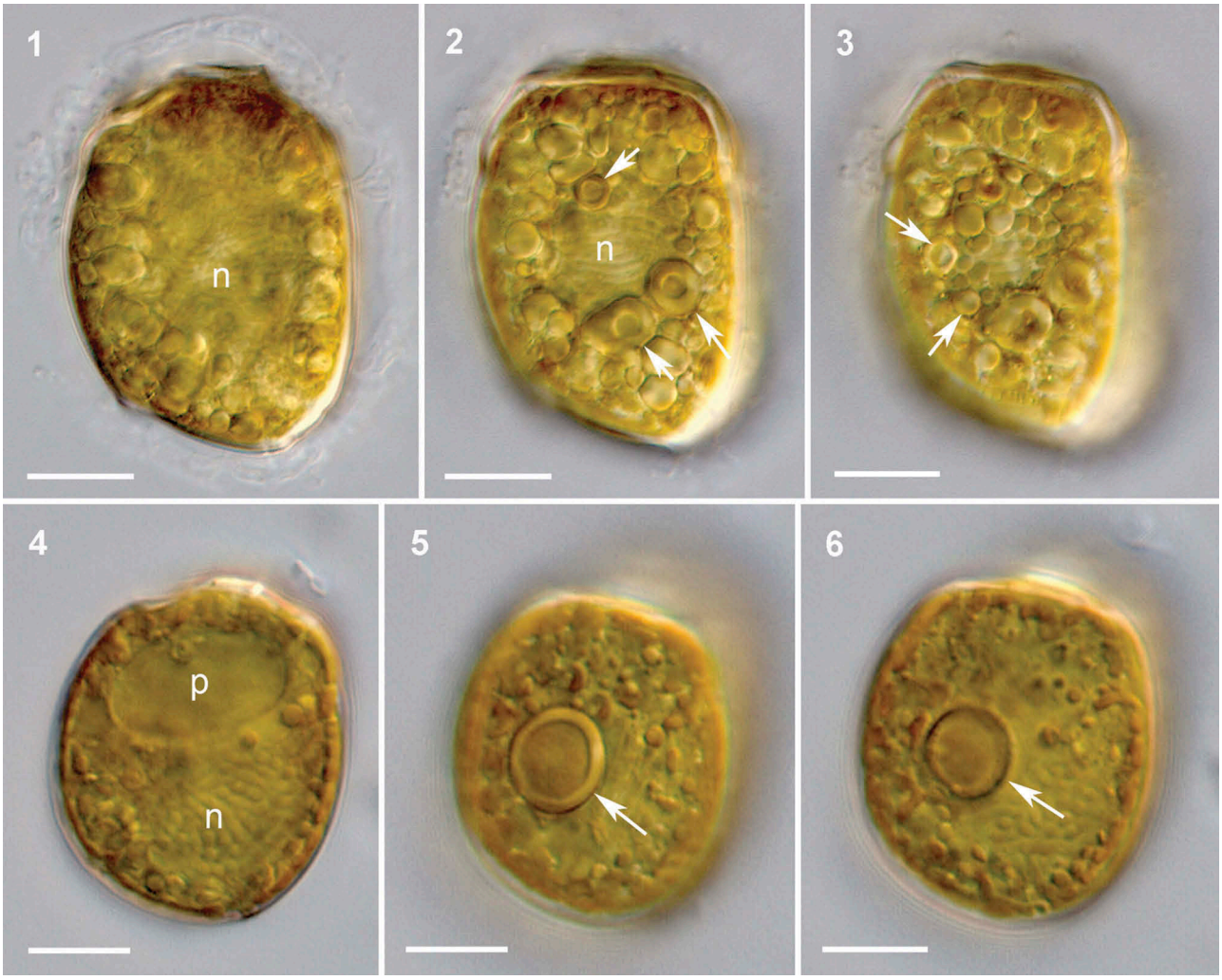

Figs 1-6. Light micrographs of *Pseudadenoides polypyrenoides* sp. nov. (1–3) and *P. kofoidii* (4–6) from Boundary Bay, Canada. **Figs 1–3**. *Pseudadenoides polypyrenoides* sp. nov., same cell in different focal planes. **Fig. 1**. Mid cell focus showing the large central nucleus (n). **Fig. 2**. Left lateral side, nucleus (n) and several pyrenoids (arrows) visible. **Fig. 3**. Additional pyrenoids (arrows) of different sizes visible. **Figs 4–6**. *Pseudadenoides kofoidii*, same cell in different focal planes. **Fig. 4**. Mid cell focus showing the posterior dorsal nucleus (n) and a large anterior pusule (p). **Figs 5, 6**. One of the two large lateral pyrenoids (arrow) visible by the starch sheath having a ring-like appearance. Scale bars = 10 μm.

(Figs 12, 16, 20, 21). The large hypotheca covered most of the cell (Figs 1–3, 7–16). The large round to oval nucleus was situated in the centre of the cell (Figs 1, 2). The cells contained brown chloroplasts and several pyrenoids with starch sheaths (starch-rings) of different diameters (Figs 2, 3). These starch-rings were not easily recognizable.

The plate formula was APC 4′ 6C 4S 5‴ 5p 1⁗ (Figs 7–12, 25–28). The epitheca consisted of five plates (Figs 17–19, 27). The apical pore complex (APC) consisted of the round to angular apical pore plate (Po) with a central apical pore, covered by a small round cover plate (cp) (Fig. 18, Supplementary Fig. 3). A small, narrow plate (canal plate X?) connected the first apical plate (1′) with either the apical pore or the cover plate by traversing the Po plate (Fig. 18, Supplementary Fig. 3). In addition to the apical pore, the Po plate had normal thecal pores arranged around the apical pore (Supplementary Fig. 3, arrows). Four apical plates of very different shapes bordered the APC (Figs 17–19). Plates 1′ and 4′ were in contact with the anterior sulcal plate (Sa) (Figs 17, 18, 27). No precingular plates were present (Fig. 27). The shallow cingulum consisted of six plates (Figs 17–19, 27). Four sulcal plates surrounded the flagellar pore (Figs 20, 21, 27, 28). The hypotheca consisted of eleven plates (Figs 7–16, 25, 26, 28). The first (1‴) and second (2‴) postcingular plates were positioned on the left lateral side of the cell; the third postcingular plate (3′ ″) was positioned on the dorsal side of the cell; and the relatively large and posteriorly pointed fourth postcingular plate (4‴) and the small fifth (5‴) postcingular plate were positioned on the right lateral side of the cell (Figs 7–16, 25, 26). Five large posterior intercalary plates made up a series that completely surrounded and covered most of the hypotheca (Figs 7–16, 25, 26, 28). The first (1p)

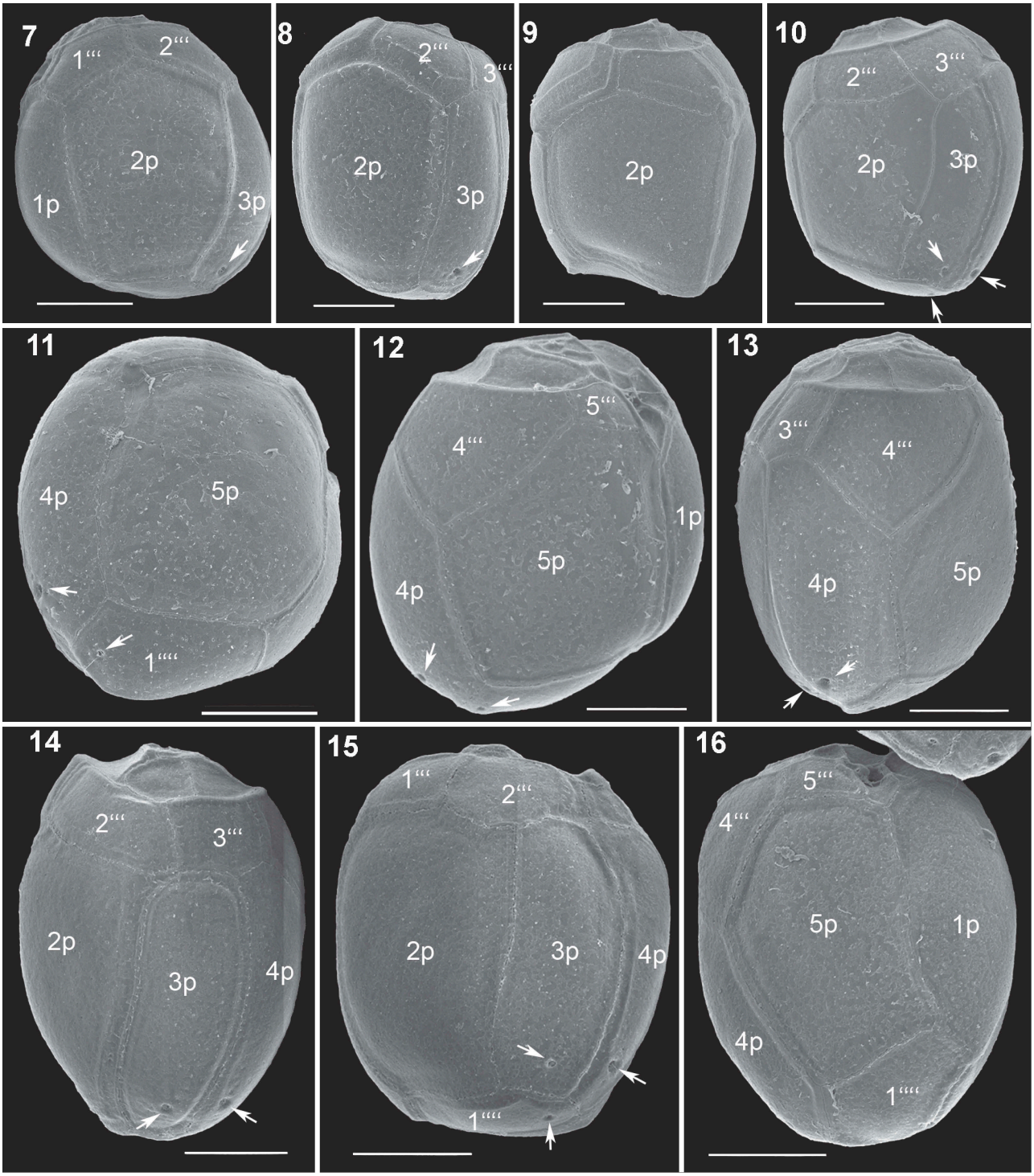

Figs 7–16. Scanning electron micrographs of *Pseudadenoides polypyrenoides* sp. nov. (culture material). **Figs 7–10**. Left lateral views. Note the posterior depressions (arrows). **Figs 11–13**. Right lateral views. Note the posterior depressions (arrows). **Fig. 14**. Dorsal view. **Fig. 15**. Left lateral to dorsal view. **Fig. 16**. Ventral view. ‴ = postcingular plate, p = posterior intercalary plate, ⁗ = antapical plate. Scale bars = 10 µm.

and fifth (5p) posterior intercalary plates contacted each other in a long ventral suture and unusually bordered the posterior sulcus (Figs 12, 16). The third (3p) and fourth (4p) posterior intercalary plates met in a long dorsal suture (Figs 14, 15). One pentagonal antapical plate (1⁗) was located at the posterior end of the cell (Figs 15, 16, 28). Three large pores with a sieve-like internal structure (Fig. 24) were present on the dorsal surface at the posterior end of the cell (Figs 10, 15, 26, 28). Plates 3p and 4p had the large pores at the posterior end, and plate 1⁗ had the large pore at the dorsal end (Figs 7–15, 28). The thecal plates were smooth with scattered pores (Figs 22–24, Supplementary Fig. 1). Wide sutures were sometimes transversally striated (Supplementary Figs 1, 2).

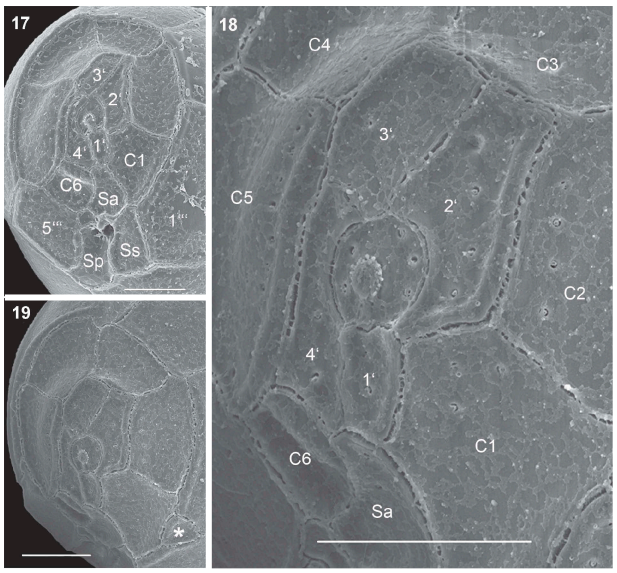

Figs 17–19. Scanning electron micrographs of *Pseudadenoides polypyrenoides* sp. nov. (culture material). **Fig. 17**. Apical view showing the epithecal, cingular and sulcal plates. **Fig. 18**. Detail of the epitheca with apical pore complex and apical plates (′). **Fig. 19**. Apical view, note the small extra plate (asterisk) between the cingular and postcingular plate series. ′ = apical plate, C = cingular plate, S = sulcal plate. Scale bars = 5 µm.

Morphological variability and plate pattern interpretations

An additional small triangular plate was observed between plates C1 and 1‴ (Fig. 19). Alternative plate pattern interpretations were possible, especially in the sulcal area. The sixth cingular plate (C6) could be a right anterior sulcal plate (Sad); if so, then the anterior sulcal plate would become a left anterior sulcal plate (Sas), and the plate formula would change to: APC 4′ 5C 5S 5‴ 5p 1⁗. Additionally, the fifth postcingular plate (5‴) could be a sulcal plate, becoming the right sulcal plate (Sd). If so, then the right sulcal plate would be changed into a middle sulcal plate (Sm), and the plate formula would change to: APC 4′ 5C 6S 4‴ 5p 1⁗ (Figs 29–32). If the posterior intercalary plates must lie between the postcingular and antapical series (neither touching the cingulum nor the sulcus) and the antapical plates must border the sulcus and not touch the cingulum, then the hypothecal plates should be named as follows: 1p = 1⁗, 2p = 1p, 3p = 2p, 4p = 3p, 5p = 2⁗, 1⁗ = 4p. If so, then the plate formula would change to: APC 4′ 6C 4S 5‴ 4p 2⁗ or APC 4′ 5C 5S 5‴ 4p 2⁗ or APC 4′ 5C 6S 4‴ 4p 2⁗ (Figs 33–36).

Ultrastructure

Cells contained a typical dinokaryon with condensed chromosomes (Figs 37, 38), trichocysts below thecal pores (Fig. 39), developing stages of trichocysts close to dictyosomes (Fig. 40), and mitochondria with tubular cristae (Fig. 41). The Golgi apparatus was located near the nucleus (Fig. 40). Dinoflagellate chloroplasts associated with several pyrenoids were distributed at the cell periphery (Figs 37, 38). The chloroplasts contained parallel thylakoids (Fig. 42) in stacks of three (Fig. 46) and had three outer membranes. Single-stalked pyrenoids were covered with a starch sheath and were partly traversed by thylakoid pairs (Figs 43–45). An electron-dense plug-like structure was positioned beneath the apical pore and was surrounded by trichocysts (Fig. 47). A membranous network, possibly belonging to the pusule, was associated with the flagellar apparatus below the flagellar pore (Fig. 48). An accumulation of trichocysts and their primordia were positioned

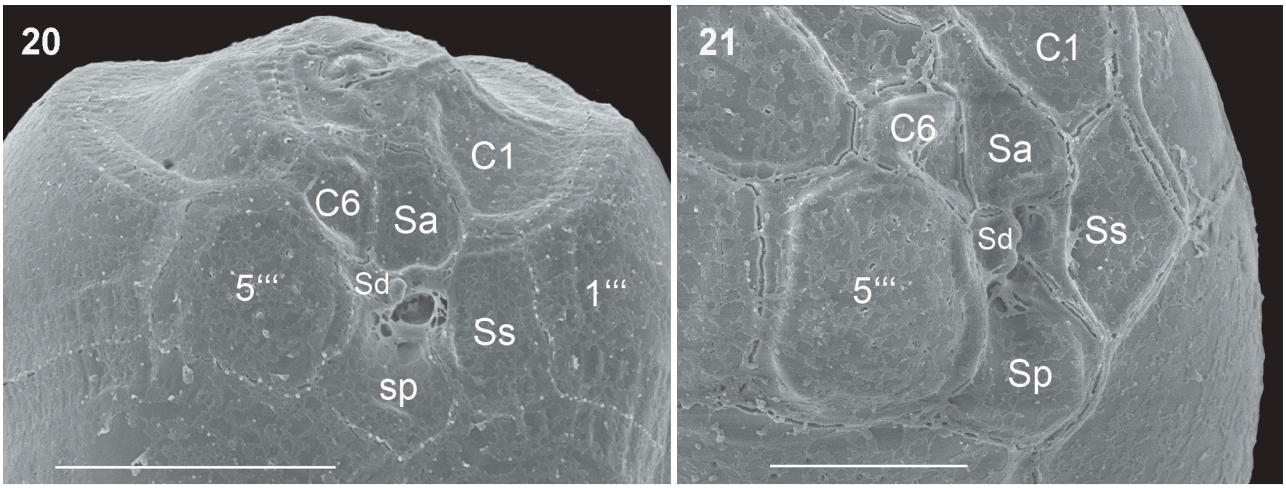

Figs 20–21. Scanning electron micrographs of *Pseudadenoides polypyrenoides* sp. nov. (culture material). **Fig. 20**. Ventral view of the anterior cell part showing the sulcus. **Fig. 21**. Right lateral to ventral view of the sulcus. C = cingular plate, ‴ = postcingular plate, Sa = anterior sulcal plate, Sd = right sulcal plate, Ss = left sulcal plate, Sp = posterior sulcal plate, Scale bars = 10 µm (20) and 5 µm (21).

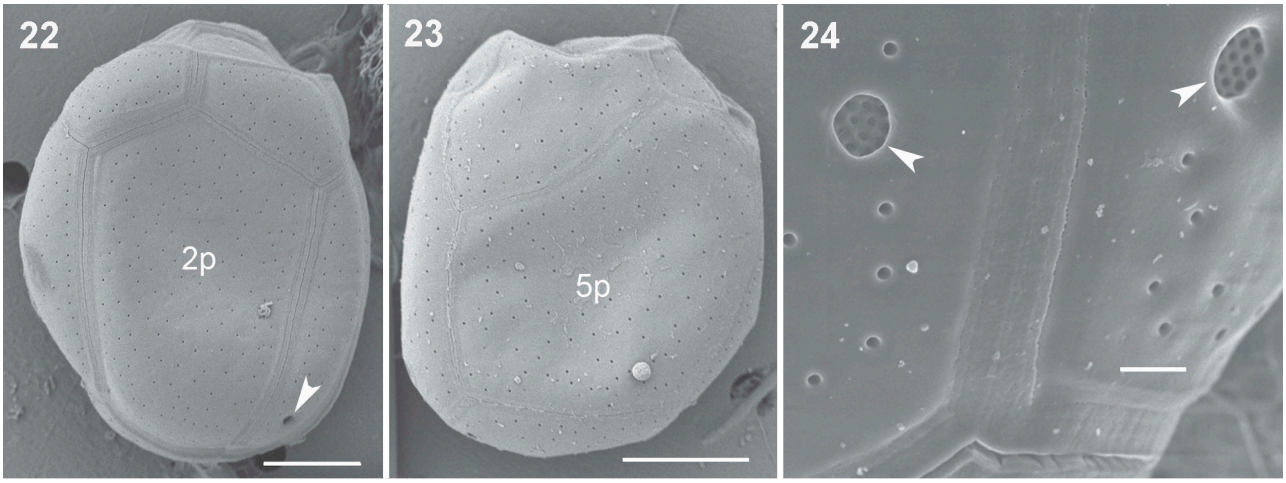

Figs 22–24. Scanning electron micrographs of *Pseudadenoides polypyrenoides* sp. nov. (cells from an environmental sample). **Fig. 22**. Left lateral cell side, with one visible posterior depression (arrowhead). **Fig. 23**. Right lateral cell side. Note the smooth thecal surface with scattered pores. **Fig. 24**. Two of the three posterior depressions with a sieve-like internal structure (arrowheads).

below the large pores with an internal sieve-like structure (Figs 49–51). Some trichocysts were observed extruding through these sieve pores (Fig. 50).

Molecular phylogenetic analyses

The phylogenetic tree inferred from SSU rDNA sequences using a maximum likelihood method demonstrated that the new species (KU726886) was a sister taxon to the *P. kofoidii* clade with high support (BP = 94 and PP = 0.99) (Fig. 52). The phylogenetic tree inferred from LSU rDNA sequences using a maximum likelihood method also showed that the new species (KU726887) formed a sister lineage to a clade comprising all *P. kofoidii* sequences from different localities (Fig. 53) with the highest statistical support (BP = 100 and PP = 1.00). The two species differed by eight bases in the SSU and 37 bases in the LSU rDNA sequences. The *P. kofoidii* clades contained *P. kofoidii* sequences (LC002843, LC002848) described by Gómez *et al.* (2015) from France plus sequences from CCMP2081 (KX000290, KX000294, Germany), CCMP1891 (KX000289, KX000293, Canada) and NIES-1367 (KX000291, KX000295, Japan) cultures from this study, which confirmed CCMP2081, 1891 and established NIES-1367 as *P. kofoidii* (Figs 52, 53). Additionally, the *P. kofoidii* clade inferred from SSU rDNA sequences (Fig. 52) contained a publicly available strain from CCCM 683 retrieved as *Adenoides eludens* (AF274249) but identified as *P. kofoidii* by Gómez *et al.* (2015). The phylogenetic positions of the SSU and LSU rDNA sequences (KX000292, KX000296) from the NIES-1402 culture (identified as *A. eludens* sensu Balech, now *P. kofoidii*) were unresolved, suggesting that this strain represents a new species of *Adenoides*, albeit with weak statistical support (Fig. 53).

Molecular phylogenetic analysis of the LSU rDNA sequences showed that the sister group to *Pseudadenoides* was a clade consisting of the new *Adenoides eludens* sequences (BP = 73 and PP = 1.00; Fig. 53). Although a clade of *Prorocentrum* taxa clustered close to the *Adenoides*/*Pseudadenoides* clade in the LSU rDNA tree (Fig. 53), this relationship did not receive statistical support in the tree inferred from SSU rDNA sequences (Fig. 52). The SSU phylogeny did not resolve the relationship between *Pseudadenoides* and *Adenoides*.

Nonetheless, the phylogenetic trees inferred from both the SSU and LSU rDNA sequence datasets demonstrated that *P. kofoidii*, *A. eludens* and *P. polypyrenoides* sp. nov. are distinct from each other.

Discussion

The most similar species to *P. polypyrenoides* sp. nov. is *P. kofoidii* (basionym: *Amphidinium kofoidii*, synonym: *Adenoides eludens* sensu Balech); both species have identical thecal tabulation patterns, a button-like epitheca, a shallow anterior cingulum, a very short sulcus, one flagellar pore, and a large hypotheca that is longer dorsally than ventrally (Balech, 1956; Hoppenrath *et al.*, 2003; Gómez *et al.*, 2015) (Table 1). In both species, the thecal plates are smooth with scattered pores. They have overlapping cell sizes but *P. polypyrenoides* is generally larger, more rectangular and more elongated in mixed environmental samples (Figs 1–6; Supplementary Table 1). The most reliable feature

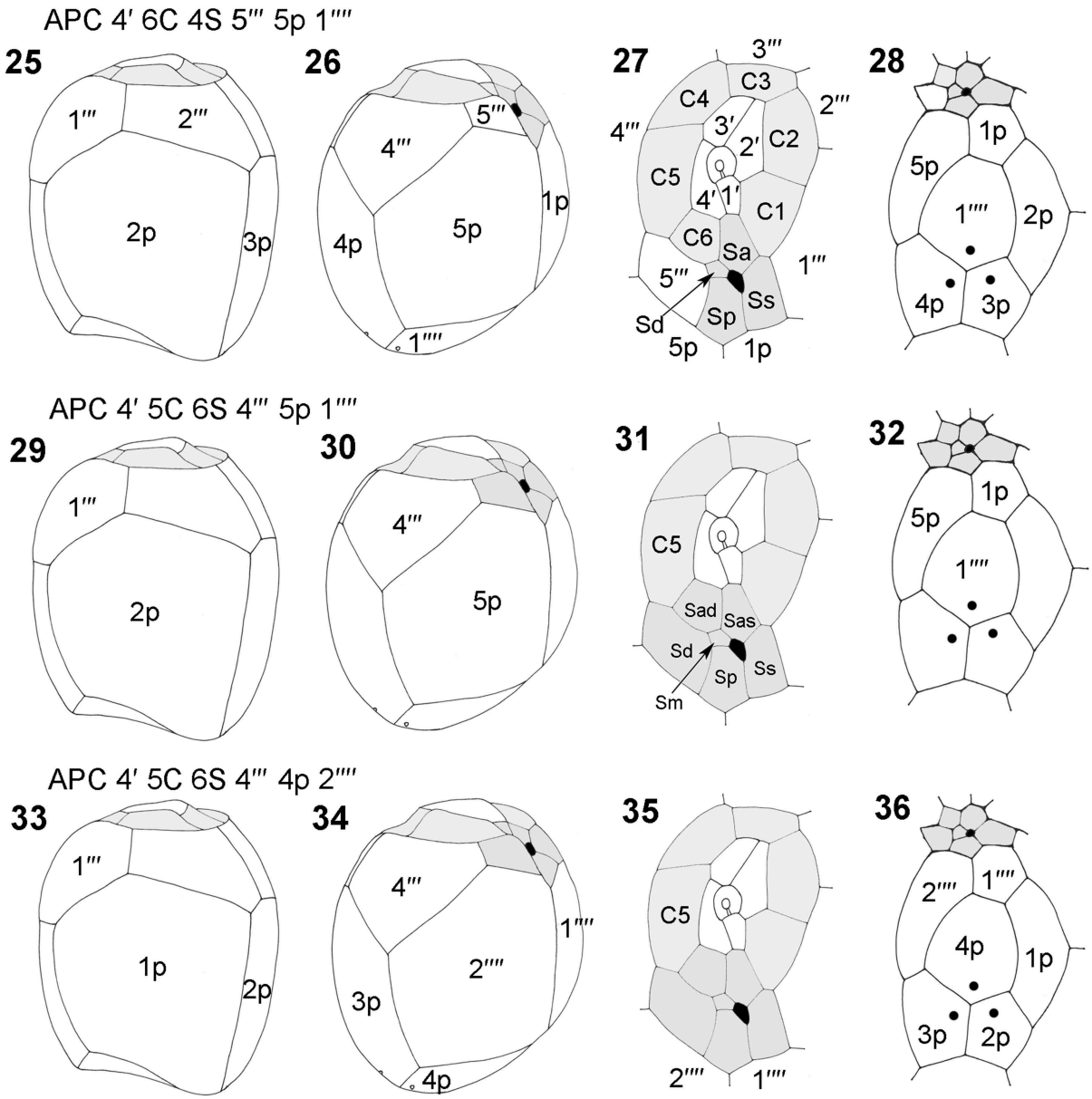

Figs 25–36. Line drawings of the theca of *Pseudadenoides polypyrenoides* sp. nov. **Figs 25–28**. Current plate pattern interpretation of the genus. **Fig. 25**. Left lateral. **Fig. 26**. Right lateral. **Fig. 27**. Epitheca and sulcus. **Fig. 28**. Partial hypotheca in antapical view. **Figs 29–32**. Alternative sulcal plate pattern and changed cingular and postcingular plate series. **Fig. 29**. Left lateral. **Fig. 30**. Right lateral. **Fig. 31**. Epitheca and sulcus. **Fig. 32**. Partial hypotheca in antapical view. **Figs 33–36**. Additional alternative hypothecal plate pattern. **Fig. 33**. Left lateral. **Fig. 34**. Right lateral. **Fig. 35**. Epitheca and sulcus. **Fig. 36**. Partial hypotheca in antapical view. 1′–4′ = apical plate series; C1–6 = cingular plate series; 1‴–5‴ = postcingular plate series; 1p–5p = posterior intercalary plate series; 1⁗(2⁗) = antapical plates; Sa = anterior sulcal plate; Sas = left anterior sulcal plate; Sad = right anterior sulcal plate; Sd = right sulcal plate; Ss = left sulcal plate; Sp = posterior sulcal plate; Sm = middle sulcal plate.

to distinguish the two species under the light microscope is the number and size of the pyrenoids; *P. kofoidii* possesses two large lateral pyrenoids (easily visible as the starch sheath appears as a ring-like structure), whereas *P. polypyrenoides* has several inconspicuous pyrenoids of different diameters distributed through the cell (Figs 1–6). The nucleus in *P. polypyrenoides* is located in the cell centre, in *P. kofoidii* in the lower dorsal cell half (Figs 1–6). Furthermore, *P. polypyrenoides* differs from *P. kofoidii* in having three large pores with an internal sieve on the dorsal side of the posterior end of the cell on plates 3p, 4p and 1⁗ (Figs 10, 15; Table 1); *P. kofoidii* has only two of these pores on plates 3p and 4p (Hoppenrath *et al.*, 2003). The two species are easily distinguishable by molecular phylogenetic analyses within a highly supported monophyletic group (Figs 52, 53).

The general ultrastructure of *P. polypyrenoides* sp. nov. is typical for dinoflagellates. One of the main differences between *P. polypyrenoides* sp. nov. and *P. kofoidii* is the size and number of

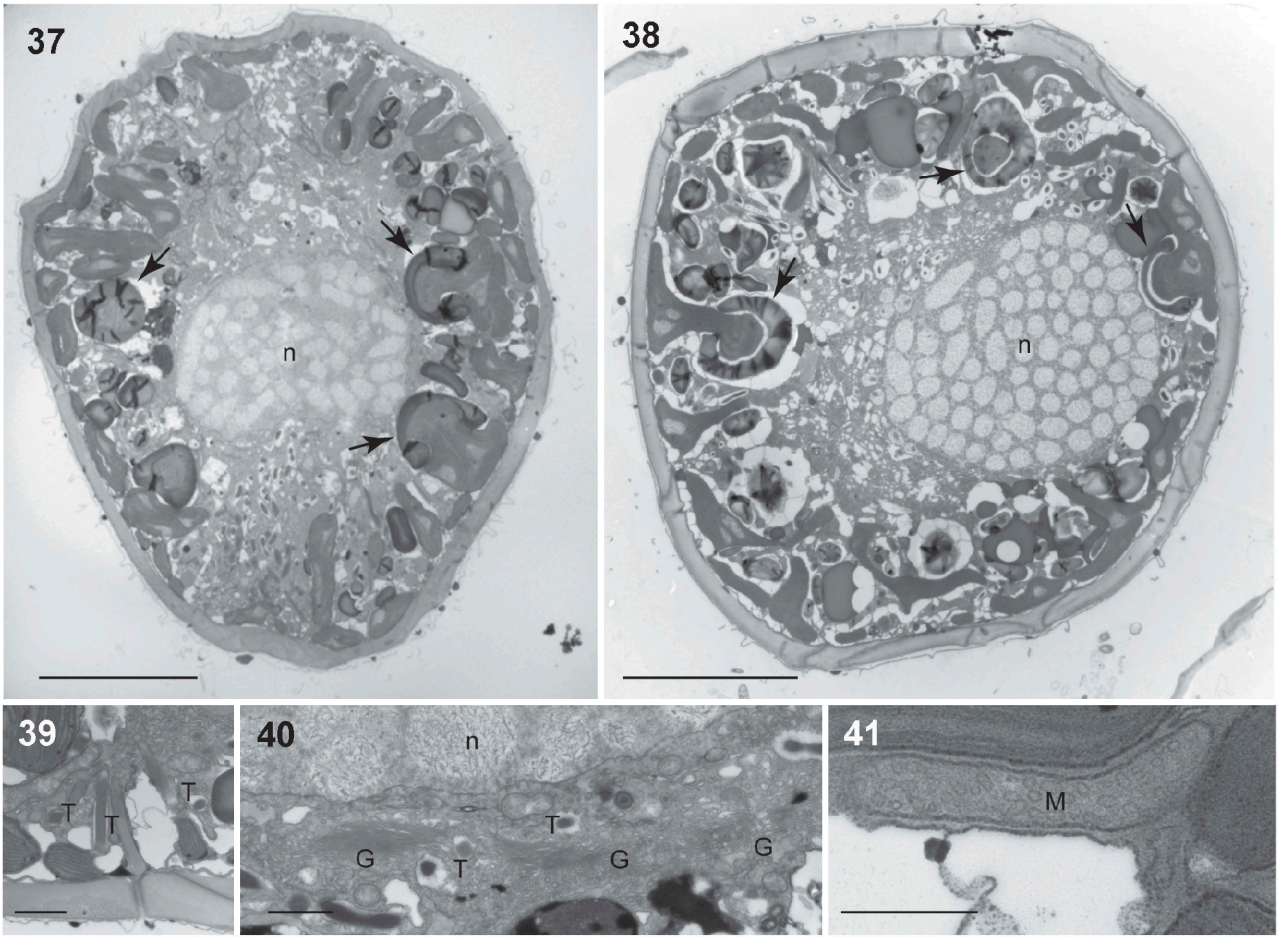

Figs 37–41. Transmission electron micrographs (TEM) showing general ultrastructural characteristics of *Pseudadenoides polypyrenoides* sp. nov. **Fig. 37**. Longitudinal image. **Fig. 38**. Transverse image through the nucleus and the pyrenoides. **Fig. 39**. Longitudinal TEM of trichocysts below a thecal pore. **Fig. 40**. High magnification TEM showing immature trichocysts adjacent to Golgi apparatus near the nucleus. **Fig. 41**. High magnification view of the mitochondrion with tubular cristae. G = Golgi body, M = mitochondrion, n = nucleus, T = trichocyst. Arrows show pyrenoids. Scale bars =10 μm (37, 38), 1 μm (39, 40), and 500 nm (41).

the pyrenoids. It has been suggested previously that pyrenoid ultrastructure is at most a species-level character, and different types of pyrenoids have been described for several dinoflagellate species (e.g. Dodge & Crawford, 1971; Hansen & Moestrup, 1998; Schnepf & Elbrächter, 1999; Hoppenrath & Leander, 2008). However, some traits associated with the pyrenoid structure can reflect phylogenetic relationships above the species level (Hansen & Moestrup, 1998). For instance, despite differences in the size and number, the pyrenoids in both species of *Pseudadenoides* share the same basic structure (i.e. single-stalked pyrenoids with internal pairs of thylakoids and external starch rings). Although single-stalked pyrenoids (type C) have been described for a few other species (e.g. *Heterocapsa rotundata* (Lohmann) Hansen, *Peridiniella catenata* (Levander) Balech), they are not common in dinoflagellates (Dodge & Crawford, 1971; Hansen, 1989; Hansen & Moestrup, 1998). Moreover, pyrenoids with internal pairs of thylakoids have also been observed in *Prorocentrum cordatum* (Ostenfeld) Dodge (as *Exuviaella mariae-lebouriae* Parke et Ballantine) and *Amphidinium carterae* Hulburt (Dodge & Crawford, 1971). Whether or not these shared traits reflect homology remains to be determined with more robust molecular phylogenetic analyses.

We also characterized traits associated with trichocysts, pusules and the apical pore region in *P. polypyrenoides* sp. nov. which are similar to those described previously in other species of dinoflagellates. The earliest stage of trichocyst ontogeny involves primordia in vesicles containing homogeneous material and a crystalline lattice (Bouck & Sweeney, 1966). Developmental stages of trichocysts were previously described in detail in *P. kofoidii* (Hoppenrath *et al.*, 2003); similar stages of trichocyst development were also evident in *P. polypyrenoides* sp. nov. (Supplementary Fig. 11). Different types of pusules have been distinguished

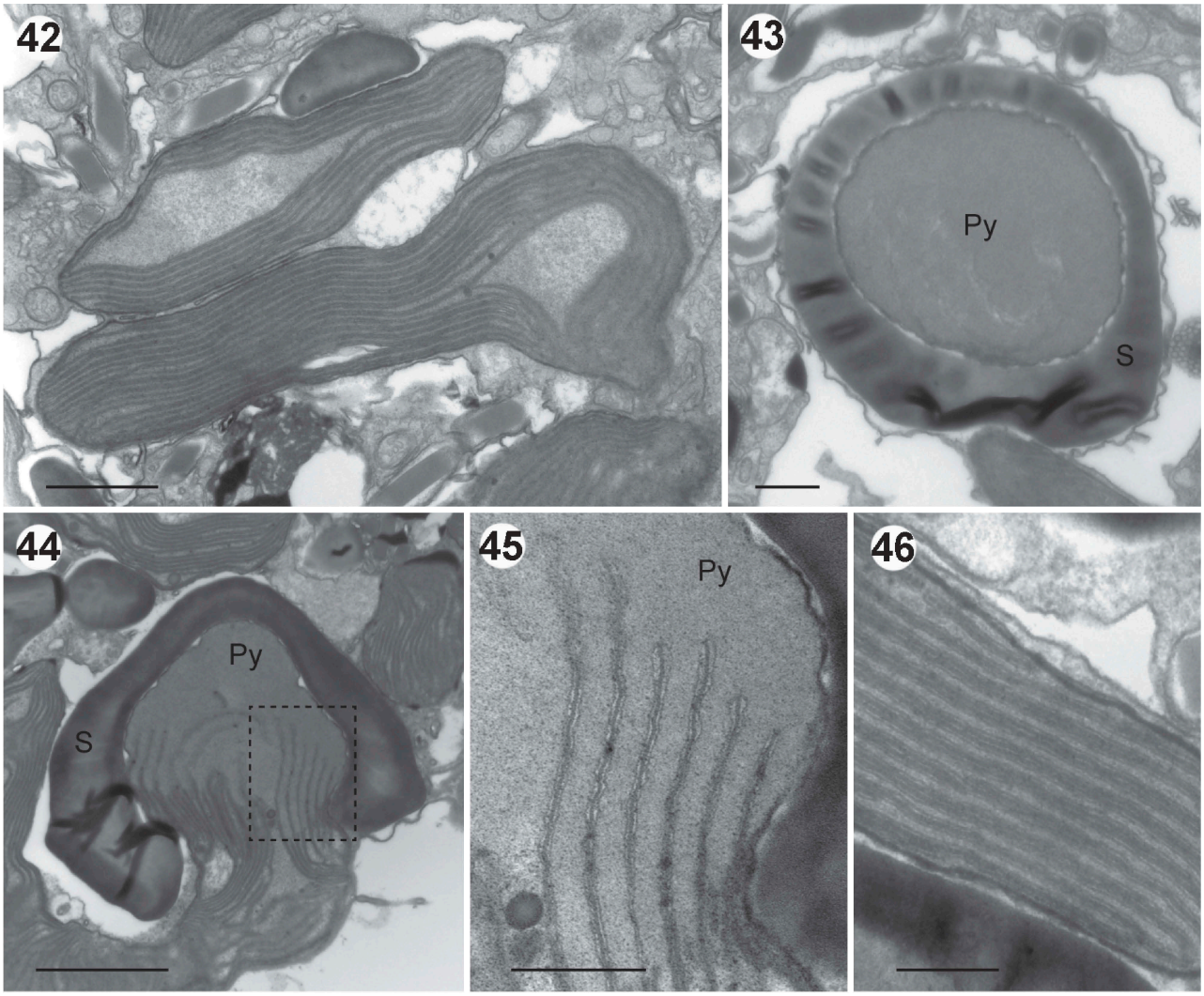

Figs 42–46. Transmission electron micrographs (TEM) showing the chloroplast and pyrenoid ultrastructure of *Pseudadenoides polypyrenoides* sp. nov. **Fig. 42**. Two chloroplasts. **Fig. 43**. Transverse TEM of the pyrenoid covered by starch sheath. **Fig. 44**. Longitudinal TEM of the pyrenoid. **Fig. 45**. High magnification view of the dotted box shown in 44. **Fig. 46**. High magnification view of the chloroplast. Py = pyrenoid, S = starch sheath. Scale bars = 1 μm (42, 43), 2 μm (44) and 500 nm (45, 46).

at the ultrastructural level (Cachon *et al.*, 1970; Dodge, 1972). The network of membranes reported here for *P. polypyrenoides* sp. nov. is interpreted to be a collapsed pusule most similar to so-called 'sack pusules' (Dodge, 1972) (Supplementary Fig. 12). Sack pusules have also been found in *Prorocentrum* species. The plug-like structure in the apical pore region described here for *P. polypyrenoides* sp. nov. is most similar to the dark-staining material in the same region in *Peridiniella catenata* (Hansen & Moestrup, 1998). Whether or not these shared traits reflect homology remains to be determined with more robust molecular phylogenetic analyses.

Both species of *Pseudadenoides* have two unusual thecal features: (1) they lack a precingular plate series, a feature only known from the benthic genus *Plagiodinium* M.A. Faust & Balech (Faust & Balech, 1993; Hoppenrath *et al.*, 2014); and (2) they have a complete posterior intercalary plate series (completely encircling the cell, the first and last posterior intercalary plates touching each other ventrally), which is novel. As described in the results, different hypothecal plate interpretations are possible when following strict definitions of posterior intercalary and antapical plates. However, the alternative pattern (4p 2′′′′) would result in antapical plates located ventrally (not reaching the antapex) and the intercalary plates not being arranged in a series, but instead arranged in a cluster. To the best of our knowledge, only one species, *Pyrophacus steinii* Schiller, is known to have a posterior intercalary plate 'cluster' (Balech, 1978).

The recently emended *Adenoides* Balech emend. F.Gómez, R.Onuma, Artigas & T.Horiguchi shows

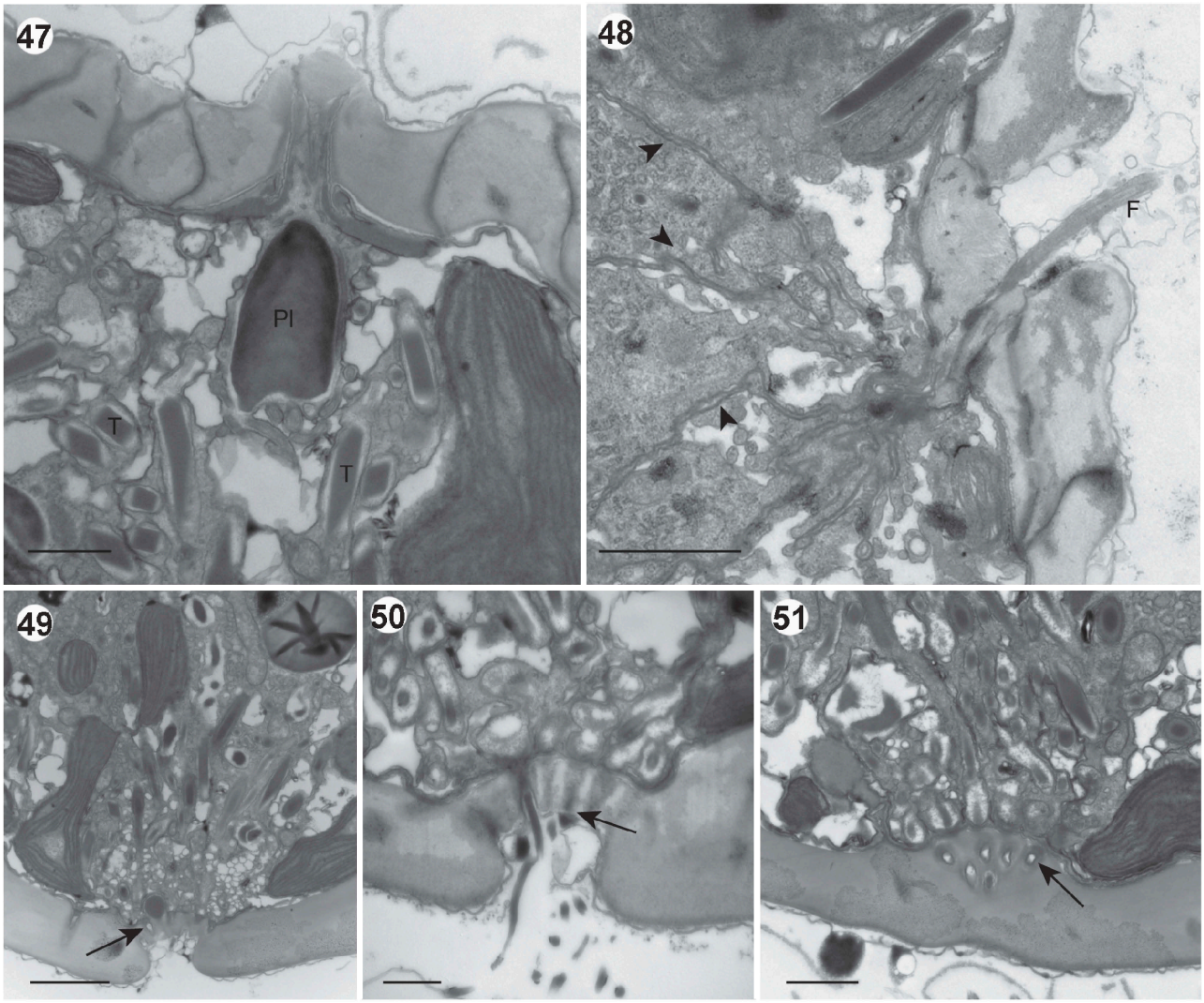

Figs 47–51. Transmission electron micrographs (TEM) of *Pseudadenoides polypyrenoides* sp. nov. **Fig. 47**. Longitudinal TEM through the apical pore. **Fig. 48**. A longitudinal section of flagellar pore. **Fig. 49**. The longitudinal sections of the posterior dorsal depression. **Fig. 50**. High magnification TEM of the posterior depressions. **Fig. 51**. Tangential TEM section of the inner sieve-like structure. F = flagellum, Pl = plug-like structure. Arrows and arrowheads indicate an inner sieve-like structure and a membrane network, respectively. Scale bars = 1 μm (47, 50, 51) and 2 μm (48, 49).

similarities with *Pseudadenoides* (Gómez *et al.*, 2015) (Table 1). The APC morphology is nearly identical to *Pseudadenoides*. Moreover, *Adenoides eludens* F.Gómez, R.Onuma, Artigas & T. Horiguchi has three distinct areas with densely arranged small pores (called 'pore fields') (Gómez *et al.*, 2015) that correspond to the three large pores with an internal sieve-plate on the dorsal side of the posterior end of *Pseudadenoides*. *Adenoides* is distinguished from *Pseudadenoides* by the possession of a precingular plate series, the lack of cingular plates, and by only three posterior intercalary plates (Hoppenrath *et al.*, 2003; Gómez *et al.*, 2015) (Table 1).

The APC construction of the two genera (Figs 57, 58) resembles *Azadinium* Elbrächter & Tillmann (e.g. Tillmann *et al.*, 2009, 2012*a*, 2014) and *Amphidoma languida* Tillmann, Salas & Elbrächter (Tillmann *et al.*, 2012*b*) (Figs 59, 60). The size and location of the canal plate (X) connecting the first apical plate with the cover plate by traversing the Po plate is special. In contrast to *Pseudadenoides* and *Adenoides*, the Po plate in *Azadinium* and *Amphidoma* is smooth without normal thecal pores. *Heterocapsa* Stein has an APC intermediate to the *Pseudadenoides*/*Adenoides* version and peridinoid APCs (Tillmann & Hoppenrath, unpubl. obs.) (Fig. 56). The *Heterocapsa* APC has a canal plate resembling peridinoid taxa (Fig. 54) but the location differs (the first apical plate has contact to Po) and an additional structure (plate?) similar to the canal plate as observed for *Pseudadenoides*/*Adenoides* (Figs 57,58). The structure has been described for

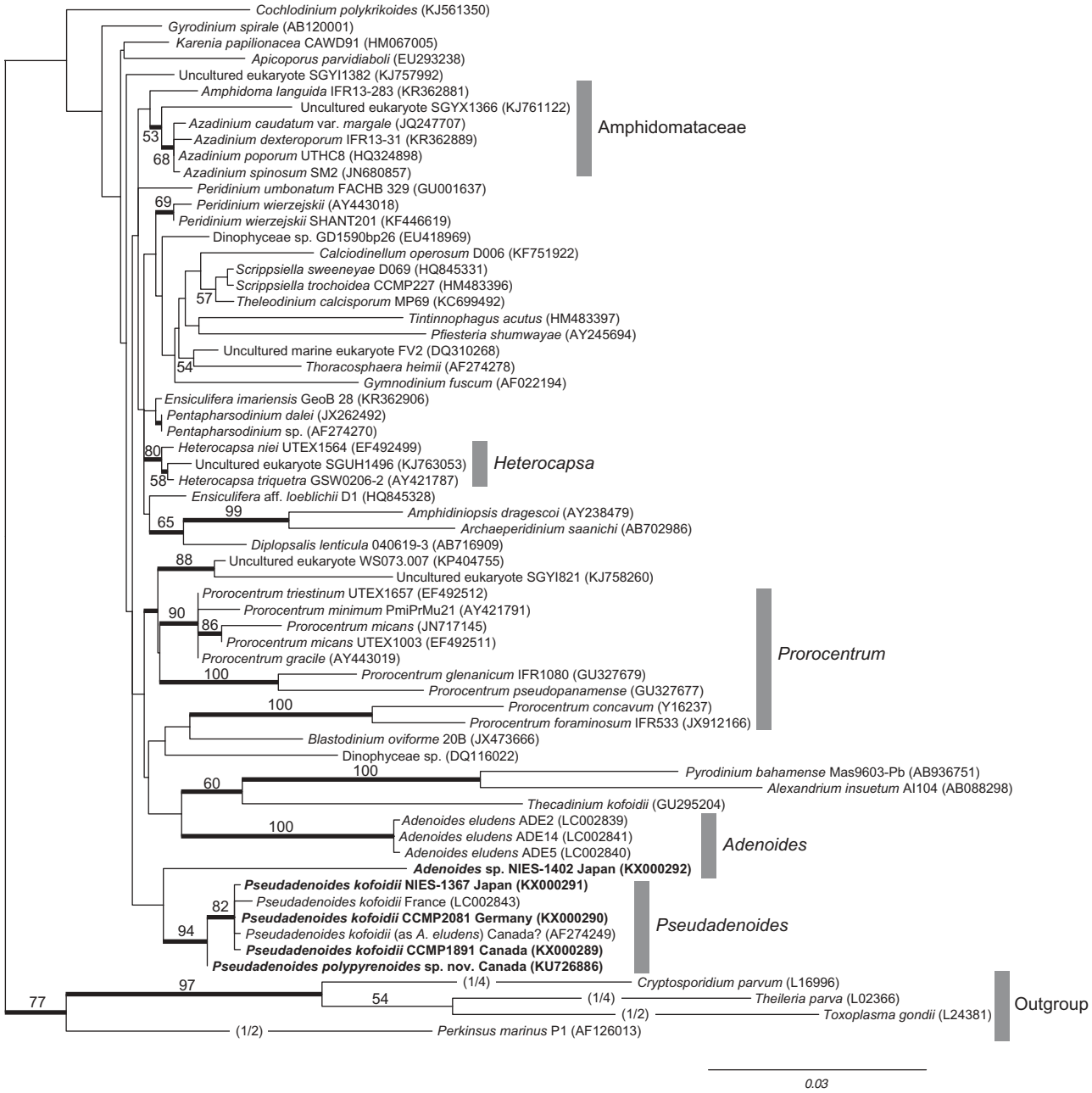

Fig. 52. Phylogenetic tree inferred from SSU rDNA sequences using a maximum likelihood model. Numbers by branches represent bootstrap support (over 50) from 1000 replicates. Bayesian posterior probabilities over 0.95 are represented by thick lines. Taxa included in this study are highlighted in bold.

Heterocapsa minima Pomroy as an extra structure acting as a hinge or connection and marked as '?' (Salas *et al.*, 2014). Tiny connecting structures between the X-plate and the cp-plate were also visible in *Azadinium* species (e.g. Tillmann *et al.*, 2014) and *Amphidoma languida* (Tillmann *et al.*, 2012*b*).

A large antapical (dorsal) pore with depressed field of small pores (= sieve plate) has been described for *Amphidoma languida* (Tillmann *et al.*, 2012*b*). Interestingly, small pore fields close to the antapical spines in some *Azadinium* species are located in a comparable region of the cell (e.g. Tillmann *et al.*, 2009, 2012*a*) and can be present also in species without an antapical spine, like *Azadinium poporum* (Tillmann *et al.*, 2016). *Azadinium* species can also have stalked pyrenoids but ultrastructural data are not available yet (e.g. Tillmann *et al.*, 2014). Another species with an antapical pore field is *Peridiniella danica* (Paulsen) Okolodkov & Dodge (Okolodkov & Dodge, 1995). Similar depressions with sieve plates and pore fields were described in a few benthic *Prorocentrum* species as well, which may be homologous with that of *Pseudadenoides* (Hoppenrath *et al.*, 2013).

The combination of morphological characters in *Pseudadenoides* overlap the traits found in both peridinioid and gonyaulacoid dinoflagellates (e.g.

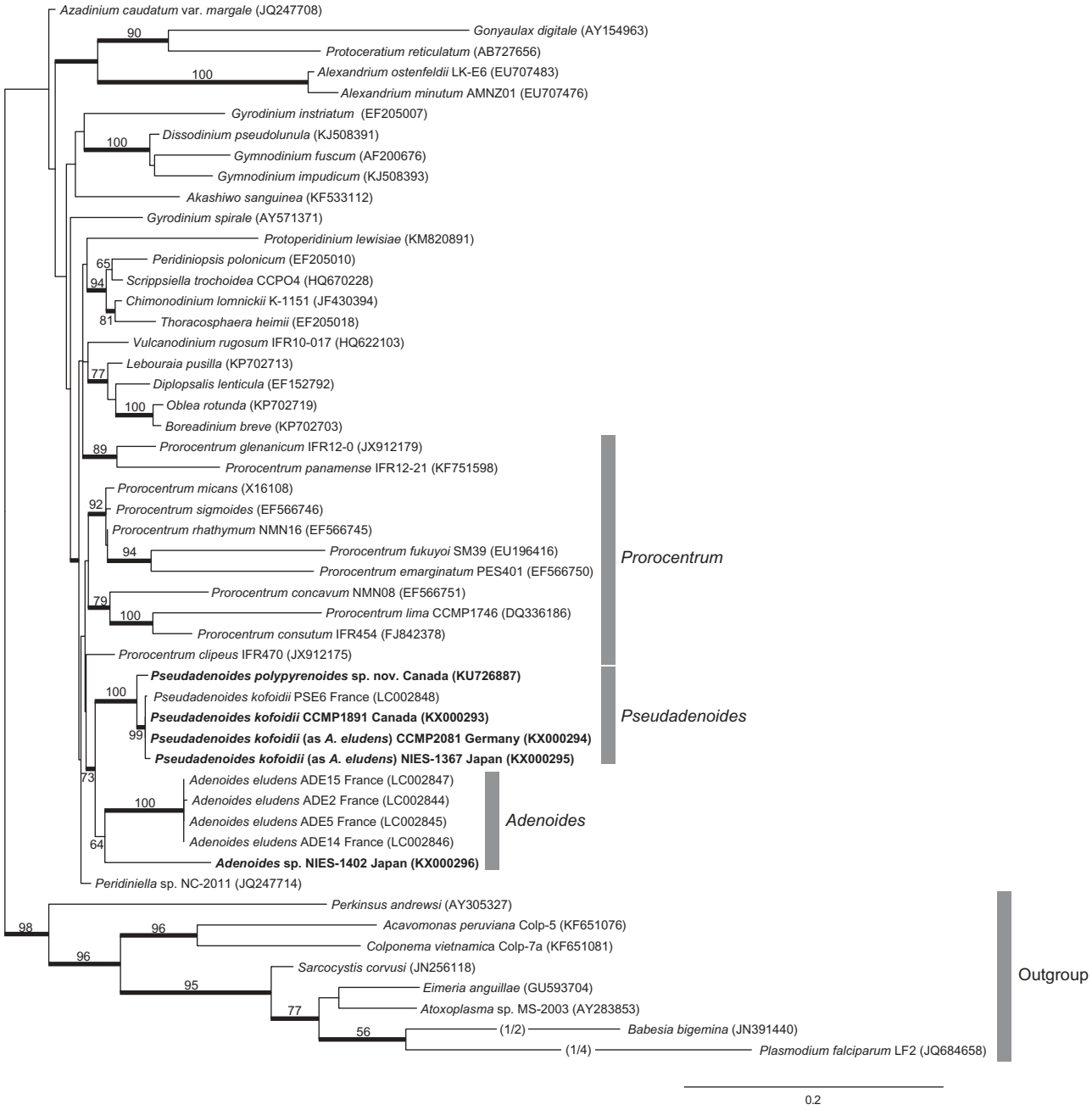

Fig. 53. Phylogenetic tree inferred from LSU rDNA sequences using a maximum likelihood model. Numbers by branches represent bootstrap support (over 50) from 1000 replicates. Bayesian posterior probabilities over 0.95 are represented by thick lines. Taxa included in this study are highlighted in bold.

the apical pore complex ultrastructure (Figs 54–60) and no clearly assignable tabulation pattern; Table 2). The genus has been placed by different authors in different orders and families (Hoppenrath *et al.*, 2003). Other genera with this combination of traits include *Azadinium, Amphidoma*, *Heterocapsa* and *Peridiniella* (Mesomorpha = *Incerta sedis* in Hoppenrath, 2016). Therefore, these taxa have an affiliation with both peridinioids and gonyaulacoids (Table 2) so are critical for understanding broad patterns of character evolution within dinoflagellates.

Gómez *et al.* (2015) treated *Pseudadenoides* and *Adenoides* as distantly related genera because of apparent evolutionary distance in their molecular phylogenetic positions. In light of the completely missing statistical support of the branches deeper in the tree, this interpretation is not supported by the data. As shown in the present study using partial LSU rDNA sequences, both genera cluster together as sister lineages with modest but compelling statistical support in the tree (Fig. 53), which is concordant with comparative morphology. The plate pattern of *Pseudadenoides* and *Adenoides* is very similar and the distinction of both genera may

Table 1. Morphological features of the *Pseudadenoides* and *Adenoides* species.

	P. kofoidii[1,3]	*P. polypyrenoides*[2]	*A. eludens*[3]
Chloroplasts	yes	yes	yes
Pyrenoids	2 large	several small	2 large
	starch sheath	starch sheath	starch sheath
Nucleus	lower dorsal cell half	cell centre	posterior
Epitheca	tiny, button-like	tiny, button-like	~1/3 cell length
Hypotheca	dorsally longer	dorsally longer	equal
Ventral hump	no	no	yes
Flagellar pore(s)	1	1	2
Cell length [µm]	30–37	29–38	27–37
Cell width [µm]		24–25	13–17
Cell depth [µm]	21–29	26–34	18–27
APC	Po, cp, X	Po, cp, X	Po, cp, X
Apical plates	4	4	5
Precingular plates	0	0	6
Cingular plates	6	6	0
Sulcal plates	4	4	3+
Postcingular plates	5	5	5
Posterior intercalary plates	5	5	3
Antapical plates	1	1	1
Thecal ornamentation	no, smooth	no, smooth	no, smooth
Pore fields posterior dorsal	2 in depression	3 in depression	3
on plates	3p, 4p	3p, 4p, 1′′′′	

[1] Hoppenrath *et al.* (2003), [2] present study, [3] Gómez *et al.* (2015).

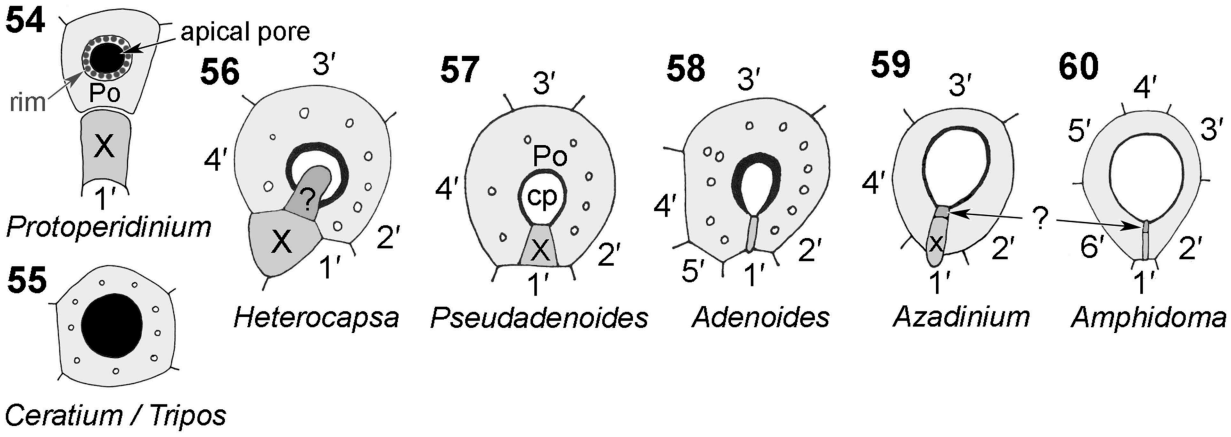

Figs 54–60. Apical pore complex (APC) construction of *Pseudadenoides*, further genera of the 'Mesomorpha' group, Peridiniales and Gonyaulacales. **Fig. 54**. *Protoperidinium* (after Dodge & Hermes 1981), Peridiniales. Dotted line = rim around the apical pore. **Fig. 55**. *Ceratium* (after Dodge & Hermes 1981), Gonyaulacales. **Figs 56–60**. Mesomorpha. **Fig. 56**. *Heterocapsa triquetra*. **Fig. 57**. *Pseudadenoides*. **Fig. 58**. *Adenoides eludens*. **Fig. 59**. *Azadinium*. **Fig. 60**. *Amphidoma languida*. Po = apical pore plate; cp (white area) = cover plate; X = canal plate; ? = a not yet described structure connecting X and cp; 1′–6′ = apical plates; black area = apical pore.

be debatable. Interpreting the plate series of *Adenoides* differently (Supplementary Figs 13–16), considering possible plate homologies, a new 'one genus hypothesis' could be formed (Supplementary Figs 13–24). It is a matter of interpretation and for the moment it is preferable to keep the separate genera (as discussed above) until further data about *Adenoides eludens* and additional *Adenoides* species become available.

The molecular phylogenetic analyses demonstrated that a culture (NIES-1402), originally identified as *Adenoides eludens* (Herdman) Balech, now *Pseudadenoides kofoidii*, most likely represents a new *Adenoides* species. The species was isolated from a beach in Wakayama, Japan, in 2003. Unfortunately, at the time it was not possible to investigate the culture in detail; the only available morphological information is light microscopic observations that show an outer shape similar to the new *A. eludens* cells and a ventral hump in the sulcal area (Supplementary Figs 4–6). In contrast to the known *A. eludens* with two large pyrenoids with starch-rings (Gómez *et al.*, 2015), the cells contain several smaller pyrenoids (Supplementary Fig. 6). These observations are consistent with the molecular data.

Table 2. Morphological features of the genera *Pseudadenoides, Adenoides, Azadinium, Heterocapsa* and characters of the dinoflagellate orders Peridiniales and Gonyaulacales (after Fensome *et al.*, 1993).

	Pseudadenoides	*Adenoides*	Peridiniales	Gonyaulacales	*Azadinium*	*Heterocapsa*
Apical pore complex (APC)	Po, cp, X symmetric small pores	Po, cp, X (a)symmetric small pores	Po, cp, X symmetric no small pores	Po, cp asymmetric small pores	Po, cp, X, ?-str. symmetric no small pores	Po, cp, X, ?-str. (a) symmetric small pores
Po in contact with 1′ plate	yes	yes	no	yes	yes	yes
First apical plate 1′	pentagonal	pentagonal hexagonal[#]	hexa-, hepta-, octa-gonal	hexagonal	hexagonal	penta-(hexa-?) gonal
First apical plate 1′ symmetry	asymmetric	asymmetric	symmetric	asymmetric	asymmetric	asymmetric
Ventral pore	no	no	no	yes	yes	no
Apical plates	4	5	4	4	4	5/4*
# anterior intercalary plates	0	0	yes (2-4)	no (0)	3	3/2*
Precingular plates	0	6	7	6	6	7/6*
Cingular plates	6	0	3–6	6	6	6
Cingulum displacement	no	n.a.	no, or weakly ascending/ descending	descending	weakly descending	weakly descending
Postcingular plates	5	5	5	6	6	5
# posterior intercalary plates	5	3	no (0)	yes (1)	0	0
Antapical plates	1′′′′	1′′′′	2′′′′ (1′′′′)	1p & 1′′′′	2′′′′	2′′′′
Antapical plates symmetry	n.a.	n.a.	symmetric	asymmetric	asymmetric	asymmetric
Flagellar pore	in contact with Sp	in contact with Sp no t & acc plates	in contact with Sp transitional plate “t”	not in contact with Sp right accessory plate	not in contact with Sp no t & acc plates	? no t & acc plates
Sulcal plates or area						
Growth bands	only on overlap- ping plate margins	?	on any plate margin	only on overlapping plate margins	only on overlapping plate margins	?
Cell division	desmoschisis	?	predominantly eleuthoroschisis	predominantly desmoschisis	desmoschisis	desmoschisis

*Type species (Tillmann & Hoppenrath unpubl. data); [#] stated in the description (Gómez et al., 2015); ? = not known; n.a. = not applicable.

Acknowledgements

We would like to thank J. McNeill, Royal Botanic Garden, Edinburgh, UK, for his advice on the nomenclatural actions that were taken to rename the genus *Adenoides* (now *Pseudadenoides*) and N. Chomérat, IFREMER Concarneau, for help with the Latin species name. We are grateful to M. Schweikert, University of Stuttgart, Germany, for discussions on the ultrastructure and U. Tillmann, AWI Bremerhaven, Germany, for discussions about the morphology of taxa with uncertain classification.

Disclosure statement

No potential conflict of interest was reported by the authors.

Funding

This work was supported by a scholarship to MH from the Deutsche Forschungsgemeinschaft (grant Ho3267/1-1) and by grants to BSL from the National Science and Engineering Research Council of Canada (NSERC 2014-05258) and the Canadian Institute for Advanced Research, Program in Integrated Microbial Biodiversity. RS was also supported by the Canadian Barcode of Life Project.

Author contributions

M. Hoppenrath: sampling, culturing, light and scanning electron microscopy, drafting and editing the manuscript; N. Yubuki: transmission electron microscopy, phylogenetic analyses, drafting and editing the manuscript; R. Stern: DNA extraction, PCR, phylogenetic analyses, editing the manuscript; B.S. Leander: infrastructure and salary support, editing the manuscript.

Supplementary Information

The following supplementary material is accessible via the Supplementary Content tab on the article's online page at http://dx.doi.org/10.1080/09670262.2016.1274788

Supplementary Table 1. Records of *Pseudadenoides* species at Boundary Bay, British Columbia, Canada.

Supplementary Figs 1–3. Scanning electron micrographs of *Pseudadenoides polypyrenoides* sp. nov. Figs 1,2. Transversely striated intercalary bands. Fig. 3. Apical pore complex consisting of the apical pore plate (Po), a cover plate (cp) and a canal plate (X). Note the normal thecal pores in the pore plate (arrows). Scale bars = 10 µm (Fig. 1) and 1 µm (Figs 2, 3).

Supplementary Figs 4–10. Light micrographs of cells from the NIES cultures represented as DNA sequences in the molecular phylogenies. Figs 4–6. NIES-1402, originally identified as *Adenoides eludens* (now *Pseudadenoides kofoidii*) and isolated from a sandy beach sample in Wakayama,

Japan. Figs 7–10. NIES-1367, originally identified as *Adenoides eludens* (now *Pseudadenoides kofoidii*) and isolated from the coast in Suzu Ishikawa, Japan. n = nucleus, p = pusule, arrows pointing at pyrenoids with starch sheath, small arrow pointing at the flagellar insertion, arrowhead pointing at a ventral hump in the sulcal area, double arrowheads pointing at the button-like epitheca. Scale bars = 10 μm.

Supplementary Figs 11–12. Transmission electron micrographs of *Pseudadenoides polypyrenoides* sp. nov. Fig. 11. Different developmental stages and sizes of trichocysts. Fig. 12. Membrane net-work of the tentative sack pusule in the collapsed condition. Scale bars = 500 nm.

Supplementary Figs 13–24. Line drawings of the theca of *Adenoides eludens* (Figs 13–16), *Pseudadenoides polypyrenoides* sp. nov. (Figs 17–20) and *Pseudadenoides kofoidii* (Figs 21–24). Figs 13, 17, 21. Left lateral. Figs 14, 18, 22. Right lateral. Figs 15, 19, 23. Apical. Figs 16, 20, 24. Antapical. 1′–5′ = apical plate series; C1–6 = cingular plate series; 1‴–5‴ = postcingular plate series; 1p–5p = posterior intercalary plate series; 1′′′′ = antapical plate; Sa = anterior sulcal plate; Ss = left sulcal plate; Sd = right sulcal plate; Sp = posterior sulcal plate;

References

Adl, S.M., Simpson, A.G.B., Lane, C.R., Lukes, J., Bass, D., Bowser, S.S., Brown, M.W., Burki, F., Dunthorn, M., Hampl, V., Heiss, A., Hoppenrath, M., Lara, E., Le Gall, L., Lynn, D.H., McManus, H., Mitchell, E.A.D., Mozley-Stanridge, S.E., Parfrey, L.W., Pawlowski, J., Rückert, S., Shadwick, L., Schoch, C.L., Smirnov, A. & Spiegel, F.W. (2012). The revised classification of eukaryotes. *Journal of Eukaryotic Microbiology*, **59**: 429–493.

Altschul, S.F., Gish, W., Miller, W., Myers, E.W. & Lipman, D.J. (1990). Basic local alignment search tool. *Journal of Molecular Biology*, **215**: 403–410.

Balech, E. (1956). Étude des dinoflagellés du sable de Roscoff. *Revue Algologique*, **2**: 29–52.

Balech, E. (1978). El genero *Pyrophacus* Stein (Dinoflagellata). *Physis*, **38**: 27–38.

Bouck, G.B. & Sweeney, B.M. (1966). The fine structure and ontogeny of trichocysts in marine dinoflagellates. *Protoplasma*, **61**: 205–223.

Cachon, J., Cachon, M. & Greuet, C. (1970). Le système pusulaire de quelques péridiniens libres ou parasites. *Protistologica*, **6**: 467–476.

Darriba, D., Taboada, G.L., Doallo, R. & Posada, D. (2012). jModelTest 2: more models, new heuristics and parallel computing. *Nature Methods*, **9**: 772.

Dodge, J.D. (1972). The ultrastructure of the dinoflagellate pusule: a unique osmo-regulatory organelle. *Protoplasma*, **75**: 285–302.

Dodge, J.D. & Crawford, R.M. (1971). A fine-structural survey of dinoflagellate pyrenoids and food-reserves. *Botanical Journal of the Linnean Society*, **64**: 105–115.

Dodge, J.D. & Hermes, H.B. (1981). A scanning electron microscopical study of the apical pores of marine dinoflagellates (Dinophyceae). *Phycologia*, **20**: 424–430.

Dodge, J.D. & Lewis, J. (1986). A further SEM study of armoured sand-dwelling marine dinoflagellates. *Protistologica*, **22**: 221–230.

Faust, M.A. & Balech, E. (1993). A further SEM study of marine benthic dinoflagellates from a mangrove island, Twin Cays, Belize, including *Plagiodinium belizeanum* gen. et sp. nov. *Journal of Phycology*, **29**: 826–832.

Fensome, R.A., Taylor, F.J.R., Norris, G., Sarjeant, W.A.S., Wharton, D.I. & Williams, G.L. (1993). A classification of living and fossil dinoflagellates. *American Museum of Natural History, Micropaleontology special publication*, **7**: 1–351.

Gómez, F., Onuma, R., Artigas, L.F. & Horiguchi, T. (2015). A new definition of *Adenoides eludens*, an unusual marine sand-dwelling dinoflagellate without cingulum, and *Pseudadenoides kofoidii* gen. & comb. nov. for the species formerly known as *Adenoides eludens*. *European Journal of Phycology*, **50**: 125–138.

Guillard, R.R.L. & Ryther, J.H. (1962). Studies of marine planktonic diatoms. I. *Cyclotella nana* Hustedt and *Detonula confervacea* Cleve. *Canadian Journal of Microbiology*, **8**: 229–239.

Hall, T.A. (1999). BioEdit: a user-friendly biological sequence alignment editor and analysis program for Windows 95/98/NT. *Nucleic Acids Symposium Series*, **41**: 95–98.

Hansen, G. (1989). Ultrastructure and morphogenesis of scales in *Katodinium rotundatum* (Lohmann) Loeblich (Dinophyceae). *Phycologia*, **28**: 385–394.

Hansen, G. & Moestrup, Ø. (1998). Light and electron microscopical observations on *Peridiniella catenata* (Dinophyceae). *European Journal of Phycology*, **33**: 293–305.

Herdman, E.C. (1922). Notes on dinoflagellates and other organisms causing discolouration of the sand at Port Erin. II. *Proceedings and Transactions of the Liverpool Biological Society*, **36**: 15–30.

Hong, D.D., Hien, H.T., Thu, N.H., Anh, H.L. & Luyen, Q. H. (2008). Phylogenetic analyses of *Prorocentrum* spp. and *Alexandrium* spp. isolated from northern coast of Vietnam based on 18S rDNA sequence. *Journal of Environmental Biology*, **29**: 535–542.

Hoppenrath, M. (2016). Dinoflagellate taxonomy – a review and proposal of a revised classification. *Marine Biodiversity*. doi: 10.1007/s12526-016-0471-8.

Hoppenrath, M. & Leander, B.S. (2008). Morphology and molecular phylogeny of a new marine sand-dwelling *Prorocentrum* species, *P. tsawwassenense* (Dinophyceae, Prorocentrales), from British Columbia, Canada. *Journal of Phycology*, **44**: 451–466.

Hoppenrath, M., Schweikert, M. & Elbrächter, M. (2003). Morphological reinvestigation and characterization of the marine, sand-dwelling dinoflagellate *Adenoides eludens* (Dinophyceae). *European Journal of Phycology*, **38**: 385–394.

Hoppenrath, M., Chomérat, N., Horiguchi, T., Schweikert, M., Nagahama, Y. & Murray, S. (2013). Taxonomy and phylogeny of the benthic *Prorocentrum* species (Dinophyceae) – a proposal and review. *Harmful Algae*, **27**: 1–28.

Hoppenrath, M., Murray, S.A., Chomérat, N. & Horiguchi, T. (2014). Marine benthic dinoflagellates – unveiling their worldwide biodiversity. Kleine Senckenberg-Reihe 54, E. Schweizerbart'sche Verlagsbuchhandlung (Nägele u. Obermiller), Stuttgart, Germany, pp 276.

Katoh, K. & Standley, D.M. (2013). MAFFT multiple sequence alignment software version 7: Improvements in performance and usability. *Molecular Biology and Evolution*, **30**: 772–780.

Katoh, K., Kuma, K., Toh, H. & Miyata, T. (2005). MAFFT version 5: improvement in accuracy of multiple

sequence alignment. *Nucleic Acids Research*, **33**: 511–518.

Lòpez-García, P., Rodrígues-Valera, F., Pedrós-Alió, C., Moreiera, D. (2001). Unexpected diversity of small eukaryotes in deep-sea Antarctic plankton. *Nature*, **409** (6820): 603–607.

Maddison, W.P. & Maddison, D.R. (2015). Mesquite: a modular system for evolutionary analysis. Version 3.04. http://mesquiteproject.org.

McNeill, J., Barrie, F.R., Buck, W.R., Demoulin, V., Greuter, W., Hawksworth, D.L., Herendeen, P.S., Knapp, S., Marhold, K., Prado, J., Prud'homme van Reine, W.F., Smith, G.F., Wiersema, J.H. & Turland, N. J. (2012). International Code of Nomenclature for Algae, Fungi, and Plants (Melbourne Code). Regnum Vegetabile 154. Koeltz, Königstein.

Okolodkov, Y.B. & Dodge, J.D. (1995). Redescription of the planktonic dinoflagellate *Peridiniella danica* (Paulsen) comb. nov. and its distribution in the N.E. Atlantic. *European Journal of Phycology*, **30**: 299–306.

Orr, R.J.S., Murray, S.A., Stüken, A., Rhodes, L. & Jakobsen, K.S. (2012). When naked became armored: an eight-gene phylogeny reveals monophyletic origin of theca in Dinoflagellates. *PLoS ONE*, **7(11)**: e50004.

Reynolds, E.S. (1963). The use of lead citrate at high pH as an electron opaque stain in electron microscopy. *Journal of Cell Biology*, **17**: 208–212.

Ronquist, F., Huelsenbeck, J. & Teslenko, M. (2011). Draft MrBayes version 3.2 manual: Tutorials and model summaries. http://mrbayes.sourceforge.net/mb3.2_manual.pdf.

Salas, R., Tillmann, U. & Kavanagh, S. (2014). Morphological and molecular characterization of the small armoured dinoflagellate *Heterocapsa minima* (Peridiniales, Dinophyceae). *European Journal of Phycology*, **48**: 413–428.

Schnepf, E. & Elbrächter, M. (1999). Dinophyte chloroplasts and phylogeny – a review. *Grana*, **38**: 81–97.

Scholin, C.A., Herzog, M., Sogin, M. & Anderson, D.M. (1994). Identification of group- and strain-specific genetic markers for globally distributed *Alexandrium* (Dinophyceae). II. Sequence analysis of a fragment of the LSU rRNA gene. *Journal of Phycology*, **30**: 999–1011.

Stern, R.F., Horak, A., Andrew, R.L., Coffroth, M.-A., Andersen, R.A., Küpper, F.C., Jameson, I., Hoppenrath, M., Véron, B., Kasai, F., Brand, J., James, E.R. & Keeling, P.J. (2010). Environmental barcoding reveals massive dinoflagellate diversity in marine environments. *PLoS ONE*, **5(11)**: e13991.

Takano, Y. & Horiguchi, T. (2006). Acquiring scanning electron microscopical, light microscopical and multiple gene sequence data from a single dinoflagellate cell. *Journal of Phycology*, **42**: 251–256.

Tillmann, U., Elbrächter, M., Krock, B., John, U. & Cembella, A. (2009). *Azadinium spinosum* gen. et sp. nov. (Dinophyceae) identified as a primary producer of azaspirazid toxins. *European Journal of Phycology*, **44**: 63–70.

Tillmann, U., Soehner, S., Nézan, E. & Krock, B. (2012a). First record of the genus *Azadinium* (Dinophyceae) from the Shetland Islands, including the description of *Azadinium polongum* sp. nov. *Harmful Algae*, **20**: 142–155.

Tillmann, U., Salas, R., Gottschling, M., Krock, B., O'Driscoll, D. & Elbrächter, M. (2012b). *Amphidoma languida* sp. nov. (Dinophyceae) reveals a close relationship between *Amphidoma* and *Azadinium*. *Protist*, **163**: 701–719.

Tillmann, U., Gottschling, M., Nézan, E., Krock, B. & Bilien, G. (2014). Morphology and molecular characterization of three new *Azadinium* species (Amphidomataceae, Dinophyceae) from the Irminger Sea. *Protist*, **165**: 417–444.

Tillmann, U., Borel, C.M., Barrera, F., Lara, R., Krock, B., Almandoz, G.O., Will, M. & Trefault, N. (2016). *Azadinium poporum* from the Argentine continental shelf, southwestern Atlantic, produces azaspirazid-2 and azaspirazid-2 phosphate. *Harmful Algae*, **51**: 40–55.

Uhlig, G. (1964). Eine einfach Methode zur Extraktion der vagilen, mesopsammalen Mikrofauna. *Helgoländer Wissenschaftliche Meeresuntersuchungen*, **11**: 178–185.

Zhang, H., Bhattacharya, D. & Lin, S. (2007). A three-gene dinoflagellate phylogeny suggests monophyly of Prorocentrales and a basal position for *Amphidinium* and *Heterocapsa*. *Journal of Molecular Evolution*, **65**: 463–474.

Zwickl, D.J. (2006). Genetic algorithm approaches for the phylogenetic analysis of large biological sequence datasets under the maximum likelihood criterion. PhD dissertation, The University of Texas at Austin.